

# VLT/FORS2 observations of four high-luminosity ULX candidates\*

M. Heida<sup>1,2</sup>, P. G. Jonker<sup>1,2,3</sup>, M. A. P. Torres<sup>1,3</sup>, T. P. Roberts<sup>4</sup>, G. Miniutti<sup>5</sup>,  
A. C. Fabian<sup>6</sup>, E. M. Ratti<sup>1</sup>

<sup>1</sup>*SRON Netherlands Institute for Space Research, Sorbonnelaan 2, 3584 CA Utrecht, the Netherlands*

<sup>2</sup>*Department of Astrophysics/IMAPP, Radboud University Nijmegen, P.O. Box 9010, 6500 GL Nijmegen, The Netherlands*

<sup>3</sup>*Harvard-Smithsonian Center for Astrophysics, 60 Garden Street, Cambridge, MA 02138, USA*

<sup>4</sup>*Department of Physics, Durham University, South Road, Durham DH1 3LE, United Kingdom*

<sup>5</sup>*Centro de Astrobiología (CSIC-INTA), Dep. de Astrofísica; ESAC, PO Box 78, E-28691, Villanueva de la Cañada, Madrid, Spain*

<sup>6</sup>*Institute of Astronomy, Madingley Road, Cambridge CB3 0HA, United Kingdom*

9 April 2018

## ABSTRACT

We obtained VLT/FORS2 spectra of the optical counterparts of four high-luminosity ( $L_X \geq 10^{40}$  erg s<sup>-1</sup>) ULX candidates from the catalog of Walton et al. (2011). We first determined accurate positions for the X-ray sources from archival *Chandra* observations and identified counterparts in archival optical observations that are sufficiently bright for spectroscopy with an 8 meter telescope. From the spectra we determine the redshifts to the optical counterparts and emission line ratios. One of the candidate ULXs, in the spiral galaxy ESO 306-003, appears to be a bona fide ULX in an HII region. The other three sources, near the elliptical galaxies NGC 533 and NGC 741 and in the ring galaxy AM 0644-741, turn out to be background AGN with redshifts of 1.85, 0.88 or 1.75 and 1.40 respectively. Our findings confirm the trend of a high probability of finding background AGN for systems with a ratio of  $\log(F_X/F_{\text{opt}})$  in the range of -1 – 1.

**Key words:** galaxies: distances and redshifts – galaxies: individual: NGC 533 – galaxies: individual: NGC 741 – galaxies: individual: AM 0644-741 – galaxies: individual: ESO 306-003 – X-rays: galaxies – X-rays: individual: CXO J064302.2-741411 – X-rays: individual: CXOU J012533.3+014642 – X-rays: individual: CXOU J015616.1+053813 – X-rays: individual: CXOU J052907.2-392458

## 1 INTRODUCTION

Ultraluminous X-ray sources (ULXs) are off-nuclear X-ray sources in galaxies with an X-ray luminosity above the Eddington luminosity of a  $10 M_\odot$  black hole, or  $\sim 10^{39}$  erg s<sup>-1</sup>. Several scenarios have been proposed to explain their high luminosities. Geometrical (King et al. 2001) or relativistic (Körding et al. 2002) beaming may allow for the observation of super-Eddington luminosities. In some sources there is evidence for a new state with truly super-Eddington accretion rates (Gladstone et al. 2009). Recent investigations into the X-ray luminosity function (XLF) of ULXs suggest that the majority of ULXs are formed by the high-luminosity tail of X-ray binaries (XRBs) and contain stellar mass black holes (BHs) (Swartz et al. 2011; Mineo et al. 2012). The best-fitting XLF exhibits a cut-off around  $10^{40}$  erg s<sup>-1</sup>, sug-

gesting that this may be the effective upper limit for the luminosity of the most massive objects in the sample.

However, Swartz et al. (2011) argue that if they extrapolate their best-fitting XLF, based on a complete sample of ULXs within 14.5 Mpc, to larger distances, they can not explain the relatively large number of ULXs with luminosities above  $10^{41}$  erg s<sup>-1</sup> that have been observed. Hence these ULXs may belong to a different class of objects. These sources would have to exceed the Eddington limit by more than a factor 100 if they contained stellar-mass black holes. They may be good candidates to host the predicted but thus far elusive intermediate-mass black holes (IMBHs). These IMBHs may form in the collapse of a dense stellar cluster (Portegies Zwart & McMillan 2002), the collapse of population III stars in the early universe (Madau & Rees 2001) or the direct collapse of massive gas clouds (Begelman et al. 2006). They may reside in globular clusters (Maccarone et al. 2007), but conclusive evidence for their existence there has not yet been found. For a review on

\* Observations based on ESO programme 088.B-0076A

IMBHs and their formation mechanisms see van der Marel (2004). The best candidate for an IMBH to date is the extremely bright source HLX-1 in ESO 243-49, which reaches maximum X-ray luminosities of  $\sim 10^{42}$  erg s $^{-1}$  (Farrell et al. 2009). The recent work by Sutton et al. (2012) provides more evidence for extreme ULXs as IMBHs.

Most ULX candidates are discovered by searching for off-nuclear X-ray point sources in galaxies (e.g. from the *Chandra* or XMM-*Newton* serendipitous source catalogs; see for example Walton et al. 2011; Liu 2011). The ULX catalogs compiled in this way are contaminated with objects that also show up as off-nuclear, bright X-ray sources but are not accreting IMBHs or stellar-mass BHs. Background active galactic nuclei (AGN) and quasars are obvious examples, but some X-ray bright supernovae (most likely type II<sub>n</sub>, Immler & Lewin 2003) and active foreground stars may also contaminate the catalogs. One way to identify these contaminants if the ULX candidate has a bright optical counterpart is to take an optical spectrum. If emission or absorption lines are present the redshift to the source can be measured. In this way we can determine whether the source is associated with the galaxy or is a background or foreground object (compare e.g. Gutiérrez 2013).

If the X-ray source is associated with the galaxy, optical spectra can give us additional information to classify the object. Some ULXs (Pakull & Mirioni 2002; Kaaret & Corbel 2009) are surrounded by bubbles of ionized gas, which can act as calorimeters and as such tell us if the emission is strongly beamed or not. The intensity ratios of the emission lines from these regions provide information on the source of the ionizing radiation, e.g. whether they are shock ionized or X-ray photo-ionized (e.g. Abolmasov et al. 2007).

We selected four high-luminosity ( $L_X \geq 10^{40}$  erg s $^{-1}$ ) ULX candidates from the catalog of Walton et al. (2011) with accurate positions that we measured using archival *Chandra* observations and optical counterparts that are sufficiently bright for optical spectroscopy. Two of the ULX candidates are situated in elliptical galaxies (NGC 533 and NGC 741). ULX candidates in elliptical galaxies have a higher chance to be background AGN (39%, compared to 24% for all sources in the catalog of Walton et al. (2011)). On the other hand, IMBHs may form in dense (globular) clusters (Portegies Zwart & McMillan 2002; Miller & Hamilton 2002) and the optical counterparts to these ULX candidates could well be just that, making them interesting targets for further investigation. AM 0644-741 is a ring galaxy with a ULX candidate situated in between the nucleus and the ring. ESO 306-003 is a spiral galaxy with a ULX in the outer edge of the disk, apparently associated with an extended optical source. We obtained optical spectra of these four sources with the FOcal Reducer and low dispersion Spectrograph (FORs2) mounted on the Very Large Telescope (VLT) (Appenzeller et al. 1998). The observations and data reduction steps are described in Section 2; Section 3 contains the results. In Section 4 we discuss our findings.

## 2 OBSERVATIONS AND DATA REDUCTION

### 2.1 X-ray observations

We use archival *Chandra* observations to get exact source positions for the ULX candidates in NGC 533, NGC 741, AM 0644-741 and ESO 306-003. Table 1 lists the details of all observations.

We use CIAO version 4.4 to process the *Chandra* observations, with the calibration files from CALDB version 4.5.0. We treat the *Chandra* observations as follows: first we update the event files with ACIS\_PROCESS\_EVENTS, then we use WAVDETECT to find the position of the ULX candidate. Sources within 3 arcmins of one of the ACIS aimpoints have a 90% confidence error circle around the absolute position with a radius of 0.6"; this is valid for the ULX candidates in NGC 533, NGC 741 and AM 0644-741. The candidate in ESO 306-003 has 25 counts and was observed at 6.6' off-axis, which means it has a 95% confidence error circle with a radius of  $\sim 1.5''$  (Hong et al. 2005). For the sources in NGC 533, NGC 741 and AM 0644-741 we extract the source counts in a circle with 6 pixel radius (90% encircled energy fraction) around the source positions using SPECEXTRACT. For the ULX candidate in ESO 306-003 we use a circle with a radius of 10 pixels to get the same encircled energy fraction, since it was observed at 6.6' off-axis. As background regions we use circles with 80 pixel radius on the same CCD but not containing any sources. We use XSPEC version 12.6.0 to fit an absorbed powerlaw (pegpwlw) to the data in the 0.3-8 keV range. We then extrapolate to get the 0.2-12 keV flux to compare this with the values reported by Walton et al. (2011). For consistency we adopt the same model parameters: a photon index of 1.7 and  $N_H = 3 \times 10^{20}$  cm $^{-2}$ , and allow only the flux to vary. We find that all *Chandra* fluxes are consistent with those from XMM-*Newton* as reported by Walton et al. (2011). The positions of the X-ray sources and their fluxes are summarized in Table 2.

### 2.2 Optical images and photometry

To find the optical counterparts of the ULX candidates we use archival optical observations of their host galaxies. NGC 533 and NGC 741 were observed as part of the Sloan Digital Sky Survey (SDSS), and we use the SDSS  $r'$ -band images to identify the optical counterparts to the ULX candidates in these galaxies (Figure 1). There is no photometric information for the source in NGC 533, so we use the aperture photometry tool in GAIA to estimate the  $r'$ -band magnitude. SDSS does provide  $u'$ ,  $g'$ ,  $r'$ ,  $i'$  and  $z'$  magnitudes for the object in NGC 741, but these are incorrect because the source is too close to the edge of the frame. Therefore we also use GAIA to estimate the  $r'$ -band magnitude for this source. For both optical counterparts we find that  $r' = 21 \pm 1$ .

The Hubble Space Telescope (HST) archive contains several observations of AM 0644-741 made with the Advanced Camera for Surveys (ACS). We use the V-band (F555W) image with exposure identifier j8my05o2q, observed on 2004-01-16 with an exposure time of 2200 seconds (see Figure 1). We visually compare the position of point sources from the USNO CCD Astrograph Catalog (UCAC)

**Table 1.** The *Chandra* observations of the four ULX candidates.

Galaxy	Observation ID	Exposure time (kiloseconds)	Source on CCD	Off-axis angle (arcmin)	Observation date (UT)
NGC 533	2880	38.1	ACIS S3	0.85	2002-07-28
NGC 741	2223	30.74	ACIS S3	2.74	2001-01-28
AM 0644-741	3969	39.97	ACIS S3	0.57	2003-11-17
ESO 306-003	4994	22.75	ACIS I3	6.60	2004-03-10

Notes: *Chandra* observation ID number, exposure time in kiloseconds, CCD on which the source was detected, the off-axis angle of the source in arcminutes and the observation date.

**Table 2.** The positions and unabsorbed 0.2-12 keV X-ray fluxes of the ULX candidates.

Host galaxy	Right Ascension	Declination	Source flux ( $\text{erg cm}^{-2} \text{s}^{-1}$ )
NGC 533	01:25:33.63	+01:46:42.6	$2.9 \pm 0.2 \times 10^{-14}$
NGC 741	01:56:16.14	+05:38:13.2	$2.5 \pm 0.3 \times 10^{-14}$
AM 0644-741	06:43:02.24	-74:14:11.1	$3.5 \pm 0.2 \times 10^{-14}$
ESO 306-003	05:29:07.21	-39:24:58.4	$2.4 \pm 0.4 \times 10^{-14}$

Notes: the positions of the ULX candidates in NGC 533, NGC 741 and AM 0644-741 are accurate to within 0.6" (90% confidence level), for the source in ESO 306-003 this value is 1.3". We fit the fluxes assuming an absorbed powerlaw with photon index 1.7 and  $N_H = 3 \times 10^{20} \text{ cm}^{-2}$  for consistency with the method used by Walton et al. (2011).

3 (Zacharias et al. 2009) with their counterparts in the HST image and find that the astrometric calibration of the image does not need to be improved. The ULX candidate has a counterpart that is in the DAOPHOT source list of this HST image in the Hubble Legacy Archive (HLA<sup>1</sup>). It has a V-band magnitude of  $21.79 \pm 0.05$ .

We identify the optical counterpart to the ULX candidate in ESO 306-003 in a 480 seconds R-band observation made on 2004-01-25 UT with VLT/VIMOS that we retrieved from the ESO archive. Its R-band magnitude is approximately 21, with the caveat that this is an extended source in a region with a very high background level due to the galaxy, which means that this measurement is not very accurate. We also obtained a  $g'$ -band, 120 seconds exposure of this galaxy in our VLT/FORS2 run (see Figure 2), of which we visually inspected the astrometric solution by comparing the positions of bright stars with those in the UCAC 3.

### 2.3 Optical spectroscopy

We obtained VLT/FORS2 observations of NGC 741 ( $3 \times 1800$  s), AM 0644-741 ( $3 \times 1800$  s) and ESO 306-003 ( $2 \times 2700$  s) on 2011-12-03 UT under programme 088.B-0076A using the GRIS\_600V grism and a 1" slit width. This configuration covers the wavelength range 4430-7370 Å with a dispersion of 0.74 Å/pixel, yielding a resolution of 4.25 Å for the 1" slit (measured at 6300 Å). This allows us to observe the H $\alpha$ , [NII] complex and the H $\beta$  and [OIII] lines if the sources are located at the same distance as their apparent host galaxies, with high enough resolution to separate them. The night was

photometric so we also observed several spectrophotometric standard stars to perform a flux calibration. The seeing varied between 0.7 and 1.1". The spectra of NGC 533 ( $3 \times 1500$  s) were made in service mode on 2012-01-16 UT with the GRIS\_300V+10 grism and a 0.5" slit width, giving a wavelength coverage from 4450-8700 Å with a dispersion of 1.68 Å/pixel and a spectral resolution of 6.4 Å for the 0.5" slit (measured at 6300 Å). The seeing varied during the night and we have no observations of spectrophotometric standards.

To reduce the spectra we use the STARLINK software package FIGARO and the PAMELA package developed by Tom Marsh<sup>2</sup>. We follow the steps outlined in the PAMELA manual to extract the spectra, using Keith Horne's optimal extraction algorithm (Horne 1986). We then use the software package MOLLY, also by Tom Marsh<sup>2</sup>, to perform the wavelength calibration and, for the data taken on 2011-12-03, the flux calibration. We do not correct for telluric absorption. Because we have multiple spectra of each source we average them to get a better signal-to-noise ratio. The two observations of ESO 306-003 were taken under varying seeing conditions. Because of this the continuum level is different in the two spectra, so we normalize these spectra before averaging them. We use MOLLY's MGFIT task to fit Gaussian profiles to the emission lines in the spectra to determine the full width at half maximum (FWHM) of the lines and the redshift to the sources.

<sup>1</sup> <http://hla.stsci.edu>

**Table 3.** Source properties of the background AGN

Source name	In galaxy	$z$	Line	FWHM km/s	$\text{Log}(F_X/F_{\text{opt}})$
CXOU J012533.3+014642	NGC 533	$1.8549 \pm 0.0003$	CIV	$2300 \pm 70$	$0.0 \pm 0.5$
			CIII]	$7800 \pm 200$	
			MgII	$5700 \pm 200$	
CXOU J015616.1+053813	NGC 741	$0.8786 \pm 0.0006$ or $1.7535 \pm 0.0009$	MgII or CIII]	$8400 \pm 200$	$0.0 \pm 0.5$
			CIII]	$5100 \pm 70$	
CXO J064302.2-741411	AM 0644-741	$1.3993 \pm 0.0001$	MgII	$4220 \pm 40$	

Notes: Lines used for the redshift determination to the quasars, their FWHM in km/s and the X-ray to optical flux ratio of these sources. The X-ray to optical flux ratios are calculated using the XMM-Newton 0.2-12 keV fluxes from Walton et al. (2011) and the  $r'$ -band (for NGC 533 and NGC 741) or V-band (for AM 0644-741) optical fluxes.

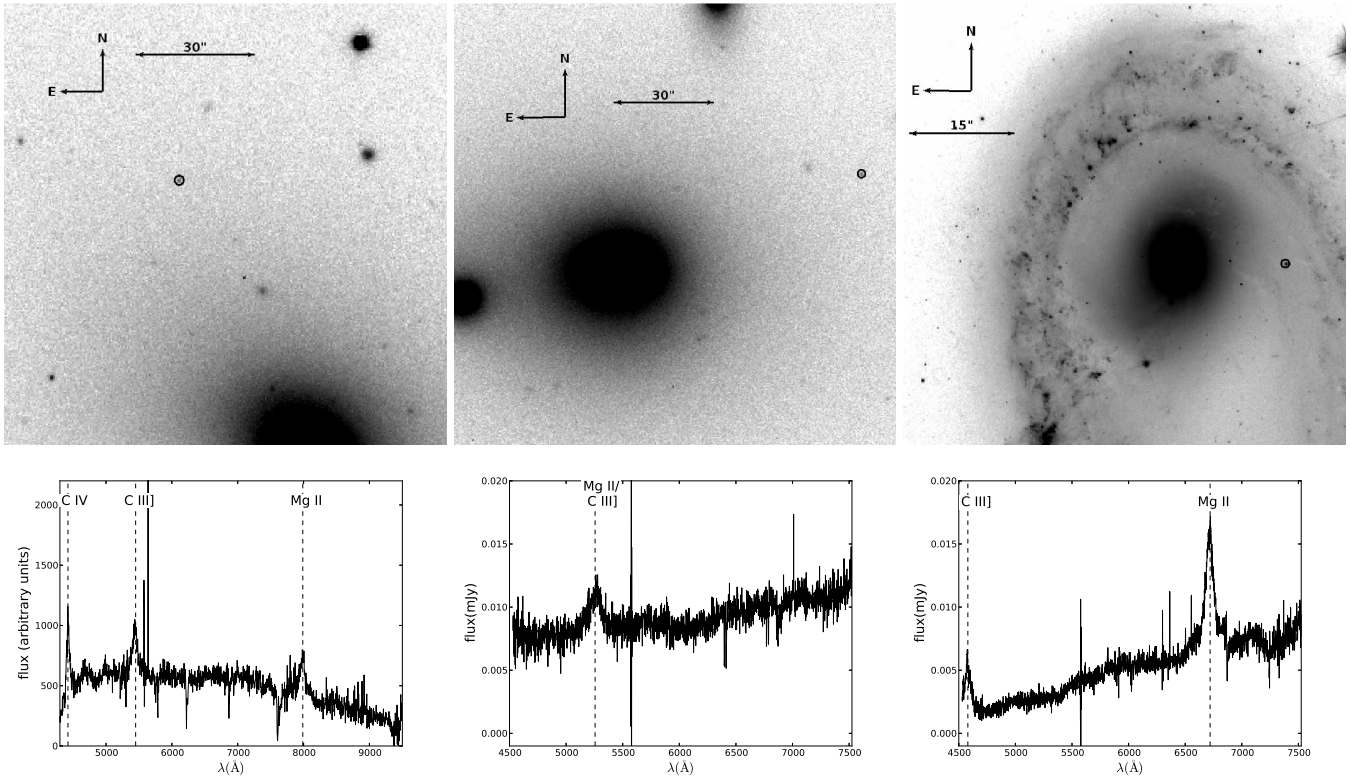


**Figure 1.** The finders and FORS2 spectra of the three ULX candidates that are background AGN. The 90% confidence error circles around the X-ray positions have a radius of  $0.6''$ , for NGC 533 and NGC 741 we plot a larger circle for visual clarity. *Left:* The SDSS  $r'$ -band image of NGC 533 with a  $1.2''$  radius circle around the *Chandra* position of the ULX candidate and the spectrum in which the CIV, CIII] and MgII emission lines, redshifted by  $z = 1.85$ , are marked. The absorption features at  $6200 \text{ \AA}$  are caused by interstellar absorption, and those at  $6900 \text{ \AA}$  and  $7600 \text{ \AA}$  are telluric in origin. *Middle:* The SDSS  $r'$ -band image of NGC 741 with a  $1.2''$  radius circle around the *Chandra* position of the ULX candidate and the spectrum of the optical counterpart. The marked emission line can be either MgII  $\lambda 2798$  line redshifted by  $z = 0.88$  or CIII] at  $z = 1.75$ . *Right:* An HST ACS V-band image of AM 0644-741 with the  $0.6''$  radius error circle around the *Chandra* position of the ULX candidate, and the spectrum with the MgII and CIII] lines, redshifted by  $z = 1.40$ , marked.

### 3 RESULTS

#### 3.1 NGC 533

NGC 533 is the dominant elliptical galaxy in a group with the same name at  $z = 0.0185$  (Smith et al. 2000). The ULX candidate is located at  $78''$  from the center of the galaxy that

has a semi-minor axis of  $90''$  (based on the D25 isophote, Nilson 1973). The X-ray source has an unresolved optical counterpart that is visible in the image of the SDSS, with  $r'$ -band magnitude  $\approx 21$ . Figure 1 shows the galaxy with the position of the ULX candidate and the FORS2 spectrum of the source.

Three broad emission lines are visible. We identify these as CIV, CIII] and MgII at  $z = 1.8549 \pm 0.0003$ . This proves

<sup>2</sup> <http://deneb.astro.warwick.ac.uk/phsaap/software>



the ULX candidate to be a background AGN, not associated with NGC 533. The 0.2-12 keV X-ray luminosity calculated for this source by Walton et al. (2011) was  $(2 \pm 1) \times 10^{40}$  erg s<sup>-1</sup>, assuming a distance to the ULX of 73.8 Mpc. The true distance to this source is 4730 Mpc (using  $H_0 = 75$  km/s/Mpc for consistency with Walton et al. 2011), which gives this AGN an X-ray luminosity of  $(7 \pm 4) \times 10^{43}$  erg s<sup>-1</sup> using the flux as measured with XMM-Newton.

### 3.2 NGC 741

NGC 741 is an elliptical galaxy located at  $z = 0.0185$  with a (D25) semi-major axis of 92.7" (de Vaucouleurs et al. 1991). The ULX candidate is located 78" West of the center of NGC 741 and has a counterpart that is unresolved in the SDSS image. Its  $r'$ -band magnitude is  $\sim 21$ . Figure 1 shows the SDSS  $r'$ -band image of NGC 741 with the position of the ULX candidate and the FORS2 spectrum of the counterpart.

The spectrum shows one broad emission line, with a FWHM of 147 Å. We cannot say with certainty which line this is. The most likely options are that it is either the MgII  $\lambda 2798$  line or the CIII]  $\lambda 1909$  line. In the first case this ULX candidate would be a background AGN at a redshift of  $z = 0.8786 \pm 0.0006$  with an X-ray luminosity of  $(1.6 \pm 0.6) \times 10^{43}$  erg s<sup>-1</sup>. In the second case it would be at  $z = 1.7535 \pm 0.0009$ , with  $L_X = (4.2 \pm 1.5) \times 10^{43}$  erg s<sup>-1</sup>. In both cases the source is not a ULX but a background AGN, unconnected to NGC 741.

### 3.3 AM 0644-741

AM 0644-741 is a ring galaxy at  $z = 0.022$  that shows signs of recent interaction with a smaller galaxy (Few et al. 1982; Lauberts & Valentijn 1989). The ULX candidate in this galaxy is located in between the core of the galaxy and the ring. A point-like object with a V-band magnitude of 21.8 is visible at the position of the X-ray source in archival HST images (see Figure 1).

The FORS2 spectrum of the counterpart shows two emission lines that we identify as MgII and CIII] at  $z = 1.3993 \pm 0.0001$ . This ULX candidate is another background AGN with an 0.2-12 keV luminosity of  $(8.1 \pm 0.8) \times 10^{43}$  erg s<sup>-1</sup>.

### 3.4 ESO 306-003

The spiral galaxy ESO 306-003, at  $z \approx 0.016$  (Couto da Silva & de Souza 2006), contains a ULX candidate that is located on the edge of the spiral structure (see Figure 2). An optical source is visible on the edge of the error circle. Visual inspection shows the profile of the counterpart to be more extended than that of point sources in the same image, but because of the high background level and steep gradient it is not possible to perform an acceptable fit to the profile. The full width at half maximum (FWHM) of point sources in this image (provided by the seeing) is 0.8". At the distance of ESO 306-003 this yields a lower limit to the size of the source of 240 pc. The two spectra that we obtained of this source show slightly different line ratios and continuum levels (for example, the  $H\beta/H\alpha$  ratio changes by 10%). This

can be explained by seeing variations if the optical counterpart to this source is extended: then slit losses can cause the small changes in the line ratios if there are intrinsic spatial variations in the line ratios in the extended source.

The spectrum is similar to that of an HII region, with narrow Hydrogen emission lines and strong forbidden lines. The redshift of the lines equals that of the center of the galaxy, indicating that if the X-rays are associated with this optical source, this is a bona fide ULX with a luminosity of  $1.4 \pm 0.3 \times 10^{40}$  erg s<sup>-1</sup> based on the XMM-Newton flux measured by Walton et al. (2011). The X-ray flux is constant between the XMM-Newton and Chandra observations. The X-ray to optical flux ratio of the source is  $\log(F_X/F_{\text{opt}}) = 0.3 \pm 0.5$ , based on the XMM-Newton 0.2-12 keV flux from Walton et al. (2011) and the  $r'$ -band flux. The line ratios, especially the [OI]  $\lambda 6300/H\alpha$  ratio, place the source among the transition objects in the diagnostic diagrams of Ho (2008) (see Figure 3). The HeII  $\lambda 4686$  emission line has been detected in several ULX nebulae (Pakull & Mirioni 2002; Kaaret & Corbel 2009), but we do not detect it here, possibly because the sensitivity of the detector drops off steeply towards the blue end. The 2- $\sigma$  upper limit for the equivalent width of this line is 1.0 Å. This corresponds to a flux of  $\sim 10^{-17}$  erg cm<sup>-2</sup> s<sup>-1</sup> or a luminosity of  $\sim 5 \times 10^{36}$  erg s<sup>-1</sup>.

## 4 DISCUSSION

We obtained VLT/FORS2 spectra of the optical counterparts of four bright ULX candidates with accurate positions obtained by us from archival Chandra observations. Two of these are located in elliptical galaxies NGC 533 and NGC 741. Another candidate is situated in AM 0644-741, a ring galaxy that recently interacted with a small elliptical galaxy, and in the spiral galaxy ESO 306-003. Three of our four targets turn out to be background AGN with X-ray luminosities ranging from 1 to  $8 \times 10^{43}$  erg s<sup>-1</sup>; one (in ESO 306-003) seems to be a bona fide ULX.

The fraction of background AGN in our sample is higher than the fraction estimated by Walton et al. (2011) for their catalog. Although this can be due to small number statistics since we only investigate four sources, it is in line with results from other spectroscopic studies of ULX candidates. Optical spectroscopy of a sample of 23 ULX candidates in total yielded 20 background AGN and three foreground stars (Gutiérrez & López-Corredoira 2005; Gutiérrez 2006; Gutiérrez & López-Corredoira 2007; Gutiérrez 2013). Another study that targeted 17 ULX candidates from the catalog of Colbert & Ptak (2002) found that 15 were background AGN and the other two objects were foreground stars Wong et al. (2008).

All these studies mainly target ULX candidates that are relatively isolated and have a bright optical counterpart, a selection effect induced by the relative ease with which spectroscopic observations can be carried out for these sources. Sources located in crowded areas, like the spiral arms of late type galaxies, are more difficult targets for ground based optical spectroscopic observations. This means that spectroscopic studies are aimed at ULX candidates that have a low X-ray to optical flux ratio and that are situated relatively far away from their suspected host galaxies. As the authors

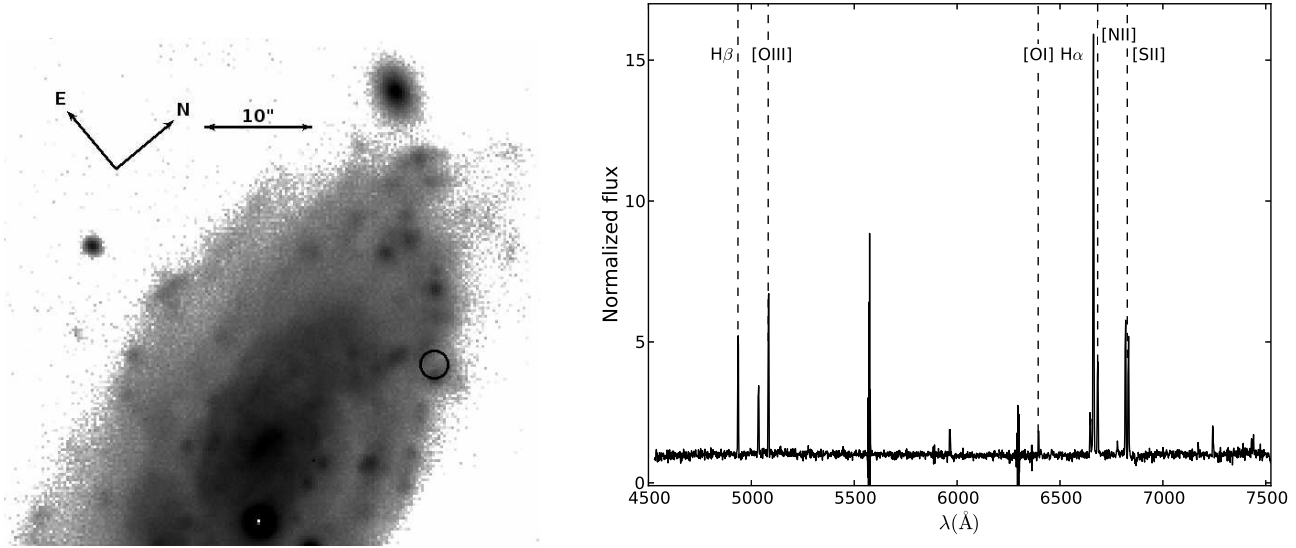


**Figure 2.** *Left:* The FORS2  $g'$ -band acquisition image of ESO 306-003 with the 1.3'' radius (90% confidence) error circle around the position of the ULX candidate. *Right:* The FORS2 spectrum of the candidate optical counterpart to the X-ray source. Several emission lines, redshifted by  $z = 0.016$ , are marked.

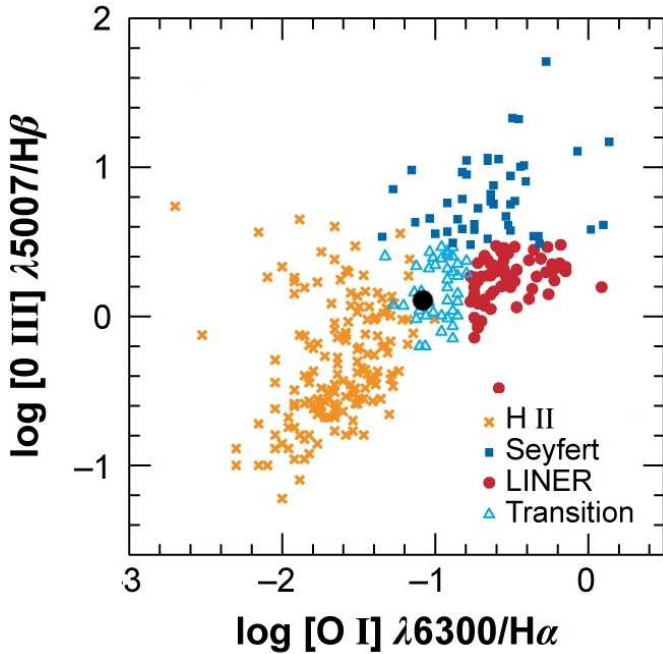


**Figure 3.**  $[\text{O III}] \lambda 5007/\text{H}\beta$  versus  $[\text{O I}] \lambda 6300/\text{H}\alpha$  line ratios for HII regions, AGN (LINERs and Seyferts) and transition objects (figure adapted from Ho 2008). The black dot represents the line ratios for the ULX in ESO 306-003.

of these previous papers also note, these selection criteria introduce a bias towards background AGN.

A possible method to select ULX candidates that are most likely to be real ULXs is to calculate the expected contribution of background sources based on the known density of AGN in X-ray and optical observations (López-Corredoira & Gutiérrez 2006; Sutton et al. 2012).

Alternatively it may be possible to use the X-ray to optical flux ratios of ULX candidates to select targets for future spectroscopic studies. All our sources have X-ray to optical flux ratios  $\log(F_X/F_{\text{opt}})$  in the range between -1 and 1, typical for AGN (e.g. Barger et al. 2003). Most ULXs show values for  $\log(F_X/F_{\text{opt}})$  ranging from 2 - 3 (Tao et al. 2011, 2012; Sutton et al. 2012). The low value that we find for the ULX in ESO 306-003 can be explained if we assume that we do not resolve the ULX counterpart but instead observe the optical flux of the entire HII region that it resides in, thus lowering  $\log(F_X/F_{\text{opt}})$ .

However, if we were to select candidates for spectroscopy on the basis of their X-ray to optical flux ratios only we run the risk of missing interesting sources. For instance, ULXs may display different values for  $\log(F_X/F_{\text{opt}})$  when observed in the high and low states, as was shown for M101 ULX-1 and M81 ULS1 (Tao et al. 2011). For both sources  $\log(F_X/F_{\text{opt}})$  is between 2 and 3 during the high state, but around 0 during the low state, well inside the range of optical to X-ray flux ratios found for AGN. Therefore other source properties should be taken into account as well, such as galaxy morphology, the distance of the ULX to its apparent host galaxy and the absolute magnitude of its optical counterpart. The source in AM 0644-741 is a good example of a candidate with such favorable properties: situated in a ring galaxy, which is a strong sign of a recent interaction phase that triggered star formation, often linked to ULXs (e.g. Swartz et al. 2004), and close to the center of its apparent host galaxy, decreasing the chance that it is a background AGN (Wong et al. 2008). It has an optical counterpart of such magnitude that it is consistent with being a bright globular cluster if it is at the distance of AM 0644-741. Nevertheless our optical spectrum showed it to be a background object.

### The ULX in ESO 306-003

The X-ray source in ESO 306-003 is the only one of the four candidates in our sample that appears to be a bona fide ULX. The extended nature of the source is confirmed by the fact that the emission line spectrum is consistent with that of an HII region. However, the [OI]/H $\alpha$  ratio indicates that some of the ionizing flux could come from an X-ray source. Potentially, we have found a ULX embedded in an HII region. Another possibility is that this ULX candidate is a background AGN shining through an HII region in ESO 306-003. The X-ray to optical flux ratio is similar to that of the other AGN in our sample, so we would expect to see a contribution of redshifted emission lines from the AGN in the optical spectrum. The fact that we do not detect this makes this scenario implausible.

We find a 2- $\sigma$  upper limit for the flux of a HeII  $\lambda$ 4686 line of  $10^{-17}$  erg cm $^{-2}$  s $^{-1}$ . This corresponds to an upper limit to the luminosity in the line of  $\sim 5 \times 10^{36}$  erg s $^{-1}$ . The presence of this line would be a strong indication of ionization by an X-ray source. We can compare this upper limit with the strength of the HeII  $\lambda$ 4686 line in other ULX nebulae. For Holmberg II X-1, Pakull & Mirioni (2002) report a luminosity of  $2.5 \times 10^{36}$  erg s $^{-1}$ . Kaaret & Corbel (2009) report a flux for this line from the ULX in NGC 5408 of  $3.3 \times 10^{-16}$  erg cm $^{-2}$  s $^{-1}$ , which translates to a luminosity of  $9 \times 10^{35}$  erg s $^{-1}$  at the distance to NGC 5408 (4.8 Mpc, Karachentsev et al. 2002). Both these ULXs have an X-ray luminosity of  $\sim 10^{40}$  erg s $^{-1}$ —similar to ESO 306-003—and a HeII  $\lambda$ 4686 to X-ray luminosity ratio of  $\sim 10^{-4}$ . If the same is true for ESO 306-003 then we would expect a HeII  $\lambda$ 4686 flux of a few times  $10^{-18}$  erg cm $^{-2}$  s $^{-1}$ , which is just below our 2- $\sigma$  upper limit. New observations of this source with greater sensitivity at the wavelength of the HeII  $\lambda$ 4686 line are needed to determine if the nebula is X-ray photo-ionized or not.

### ACKNOWLEDGEMENTS

PGJ and MAPT acknowledge support from the Netherlands Organisation for Scientific Research. GM acknowledges support from the Spanish Plan Nacional de Astronomía y Astrofísica under grant AYA2010-21490-C02-02. This research is based on observations made with ESO Telescopes at the La Silla Paranal Observatory under programme ID 088B-0076A. This research has made use of software provided by the Chandra X-ray Center (CXC) in the application package CIAO and of the software packages Pamela and Molly provided by Tom Marsh.

### REFERENCES

Abolmasov, P., Fabrika, S., Sholukhova, O., Afanasiev, V., 2007, *Astrophysical Bulletin*, 62, 36  
 Appenzeller, I., et al., 1998, *The Messenger*, 94, 1  
 Barger, A. J., et al., 2003, *AJ*, 126, 632  
 Begelman, M. C., Volonteri, M., Rees, M. J., 2006, *MNRAS*, 370, 289  
 Colbert, E. J. M., Ptak, A. F., 2002, *ApJS*, 143, 25  
 Couto da Silva, T. C., de Souza, R. E., 2006, *A&A*, 457, 425

de Vaucouleurs, G., de Vaucouleurs, A., Corwin, Jr., H. G., Buta, R. J., Paturel, G., Fouqué, P., 1991, *Third Reference Catalogue of Bright Galaxies*. Volume I: Explanations and references. Volume II: Data for galaxies between 0 $^h$  and 12 $^h$ . Volume III: Data for galaxies between 12 $^h$  and 24 $^h$ .  
 Farrell, S. A., Webb, N. A., Barret, D., Godet, O., Rodrigues, J. M., 2009, *Nature*, 460, 73  
 Few, J. M. A., Arp, H. C., Madore, B. F., 1982, *MNRAS*, 199, 633  
 Gladstone, J. C., Roberts, T. P., Done, C., 2009, *MNRAS*, 397, 1836  
 Gutiérrez, C. M., 2006, *ApJ*, 640, L17  
 Gutiérrez, C. M., 2013, *A&A*, 549, A81  
 Gutiérrez, C. M., López-Corredoira, M., 2005, *ApJ*, 622, L89  
 Gutiérrez, C. M., López-Corredoira, M., 2007, *A&A*, 472, 87  
 Ho, L. C., 2008, *ARA&A*, 46, 475  
 Hong, J., van den Berg, M., Schlegel, E. M., Grindlay, J. E., Koenig, X., Laycock, S., Zhao, P., 2005, *ApJ*, 635, 907  
 Horne, K., 1986, *PASP*, 98, 609  
 Immler, S., Lewin, W. H. G., 2003, in K. Weiler, ed., *Supernovae and Gamma-Ray Bursters*, vol. 598 of *Lecture Notes in Physics*, Berlin Springer Verlag, p. 91  
 Kaaret, P., Corbel, S., 2009, *ApJ*, 697, 950  
 Karachentsev, I. D., et al., 2002, *A&A*, 385, 21  
 King, A. R., Davies, M. B., Ward, M. J., Fabbiano, G., Elvis, M., 2001, *ApJ*, 552, L109  
 Körding, E., Falcke, H., Markoff, S., 2002, *A&A*, 382, L13  
 Lauberts, A., Valentijn, E. A., 1989, *The surface photometry catalogue of the ESO-Uppsala galaxies*, Garching, European Southern Observatory  
 Liu, J., 2011, *ApJS*, 192, 10  
 López-Corredoira, M., Gutiérrez, C. M., 2006, *A&A*, 454, 77  
 Maccarone, T. J., Kundu, A., Zepf, S. E., Rhode, K. L., 2007, *Nature*, 445, 183  
 Madau, P., Rees, M. J., 2001, *ApJ*, 551, L27  
 Miller, M. C., Hamilton, D. P., 2002, *MNRAS*, 330, 232  
 Mineo, S., Gilfanov, M., Sunyaev, R., 2012, *MNRAS*, 419, 2095  
 Nilson, P., 1973, *Nova Acta Regiae Soc. Sci. Upsaliensis Ser. V*, 0  
 Pakull, M. W., Mirioni, L., 2002, *ArXiv*: 0202488  
 Portegies Zwart, S. F., McMillan, S. L. W., 2002, *ApJ*, 576, 899  
 Smith, R. J., Lucey, J. R., Hudson, M. J., Schlegel, D. J., Davies, R. L., 2000, *MNRAS*, 313, 469  
 Sutton, A. D., Roberts, T. P., Walton, D. J., Gladstone, J. C., Scott, A. E., 2012, *MNRAS*, 423, 1154  
 Swartz, D. A., Ghosh, K. K., Tennant, A. F., Wu, K., 2004, *ApJS*, 154, 519  
 Swartz, D. A., Soria, R., Tennant, A. F., Yukita, M., 2011, *ApJ*, 741, 49  
 Tao, L., Feng, H., Grisé, F., Kaaret, P., 2011, *ApJ*, 737, 81  
 Tao, L., Feng, H., Kaaret, P., Grisé, F., Jin, J., 2012, *ApJ*, 758, 85  
 van der Marel, R. P., 2004, in “Coevolution of Black Holes and Galaxies”, *Carnegie Observatories Astrophysics Series*; Cambridge University Press; L.C. Ho, Ed., 37  
 Walton, D. J., Roberts, T. P., Mateos, S., Heard, V., 2011, *MNRAS*, 416, 1844

Wong, D. S., Chornock, R., Filippenko, A. V., 2008, *PASP*,  
120, 266

Zacharias, N., et al., 2009, Third U.S. Naval Observatory  
CCD Astrograph Catalog (UCAC3), *VizieR Online Data  
Catalog I/315*, 0